Talanta 201 (2019) 295–300

Contents lists available at ScienceDirect

Talanta

journal homepage: www.elsevier.com/locate/talanta

A novel electrochemical sensor based on carbon nanotubes array for selective detection of dopamine or uric acid

Yang Yang, Meixian Li, Zhiwei Zhu*

Beijing National Laboratory for Molecular Sciences, College of Chemistry and Molecular Engineering, Peking University, Beijing, 100871, PR China

ARTICLE INFO

Keywords:
Carbon nanotubes array
Electrochemical sensor
Dopamine
Uric acid
Ascorbic acid

ABSTRACT

A novel single-walled carbon nanotubes array-modified glassy carbon electrode (SWCNTs array-GCE) has been fabricated through a simple electrochemical technique. Benefitting from their vertically aligned configuration on the electrode surface, the modified single-walled carbon nanotubes can be used more efficiently in comparison with other modified method. The as-fabricated SWCNTs array-GCE can separate the anodic oxidation potential of dopamine (DA), uric acid (UA) and ascorbic acid (AA) with well-defined peak separation in the presence of each other, and thus employs as a new electrochemical sensor for selective determination of DA and UA. It can make a further improvement of the electrocatalytic ability of the electrode to perform an acetone pretreatment to SWCNTs array-GCE before electrochemical detection, which has been confirmed by atomic force microscope and electrochemical impedance spectroscopic measurements. Especially, unlike other carbon nanotubes-based electrode at which only two redox pairs are observed for dopamine oxidations, a third two-electron oxidation of 5,6-dihydroxyindole to indole-5,6-quinone can be clearly observed at acetone-pretreated SWCNTs array-GCE, showing the excellent electrocatalytic performance of as-fabricated electrode toward dopamine. The practicability of SWCNTs array-GCE was evaluated for the selective detection of DA and UA in real sample solutions of human serum and urine. It revealed acceptable recovery results in the range of 94–104%, indicating that it might be a promising platform for further biosensor development.

1. Introduction

Dopamine (DA), uric acid (UA) and ascorbic acid (AA) are compounds of great biomedical interest, playing key roles in the human metabolism, central nervous and renal systems [1,2]. Generally, DA and AA coexist in extracellular fluid while UA and AA coexist in blood and urine [2]. Abnormal DA level can manifest several neurological disorders. For example, Parkinsonism and schizophrenia are linked to the release of low and high DA level, respectively [3]. High UA level is one of the symptoms of some diseases such as gout and hyperuricemia, while the deficiency of AA can cause such diseases like scurvy [4]. Therefore, the early and easy sensing of these biomolecules is of significance in physiology research, disease diagnosis and drug research. Owing to their redox activity, various electrochemical techniques have been developed for their detection and analysis [5–7]. However, their electrochemical quantification at traditional electrodes encounters two major problems, one is the electrode fouling upon oxidation, and the other is the interference among them due to their overlapping of the oxidation potentials, resulting in poor selectivity and reproducibility [8]. Tremendous efforts have been made to solve these problems including various surface modifications on the electrode, new materials for making the electrodes, new electrochemical techniques and even nonoxidative electrochemical sensor [9]. Among these methods, the feasibility to modify the electrode with different molecules having inherent electrocatalytic activity has made it extremely useful in discriminating DA and its interfering AA or UA [10–17].

In particular, there have been many reports suggesting that carbon nanotubes (CNTs) promote certain types of electron-transfer reaction, minimize surface fouling and enhance electrocatalytic activity. CNTs modified electrodes have been reported to detect DA, AA and UA with significantly improved selectivity and sensitivity [14,18–21]. Basically, the biggest obstacle to hinder the use of CNTs in the field of modified electrode is the difficulty in dispersing pristine CNTs to form stable solutions, resulting from their low solubility in most common polar and apolar solvents. Functionalizing or compositing CNTs with other materials has become a good option [22]. But the frequently used modifying method such as drop-casting would give rise to another problem that the random orientation of CNTs on the electrode surface limits exposure of active sites, leading to a low efficiency of CNTs [23]. Obviously, the ordered CNTs array should improve the electrochemical

* Corresponding author.
E-mail address: zwzhu@pku.edu.cn (Z. Zhu).

https://doi.org/10.1016/j.talanta.2019.03.096
Received 23 December 2018; Received in revised form 18 March 2019; Accepted 28 March 2019
Available online 02 April 2019
0039-9140/

responses and detection performance due to their highly ordered structure and excellent catalytic activity [24,25].

Nevertheless, how to make CNTs be aligned as much as possible onto the electrode surface remains a major challenge. Several approaches have been made to overcome this problem, including chemical vapor deposition (CVD), covalent bonds connection (CBC) and self-assembly (SA). CVD can make CNTs grow vertically on the silicon substrates, but the indispensable high temperature also brings about difficulty to control [26]. The strategy of CBC is connecting the carboxylated CNTs onto the substrate by covalent bond such as Au—S, Si—O, amide bond and so on. The drawbacks of this method lie in complication and even anhydrous oxygen-free environment [27–29]. SA is a good approach but very time-consuming [30,31].

In our previous paper, we reported a facile electrochemical method to fabricate a monolayer CNTs array, which is attached orderly to the oxidized surface of GCE with ethylenediamine (EDA) as a double peptide bond linker [32]. Here, we conducted a further optimization to this method, especially in terms of the fabrication of an electrochemical sensor for simultaneous detection of DA and UA. Interestingly, a third two-electron oxidation of 5,6-dihydroxyindole to indole-5,6-quinone during DA oxidations can be clearly observed at the as-prepared modified electrode, and that is just one of major reasons why AA cannot be accurately quantitated by this sensor.

2. Materials and methods

2.1. Apparatus

Electrochemical measurements were conducted with a CHI 660A electrochemical workstation (China). The three-electrode system contains a glassy carbon electrode (GCE, 3 mm in diameter) or modified GCE as working electrode, a platinum foil (6 × 2 mm) as auxiliary electrode and a saturated calomel electrode (SCE) as reference electrode. Cyclic voltammetry (CV) and Square wave voltammetry (SWV) experiments were carried out using 0.1 M phosphate buffer solution (PBS, pH 7.4) as the supporting electrolyte unless otherwise stated. Electrochemical impedance spectroscopy (EIS) was conducted in the frequency range of 0.1 Hz–100 kHz at an initial potential of −1 mV and an amplitude of 5 mV. The electrolyte was 0.1 M KCl containing 5 mM K_3 [$Fe(CN)_6$]/K_4 [$Fe(CN)_6$]. Atomic force microscope (AFM) characterization was taken using Dimension Icon (Bruker AXS GmbH, Germany) operated under tapping mode in ambient atmosphere, and the images were taken with a scan rate of 1 Hz and the resolution of 256 lines/sample.

2.2. Reagents

SWCNTs (0.7–0.9 nm in diameter) were purchased from Nanjing JC Nano Technology Co. Ltd. (China). The carboxylated SWCNTs were prepared as follows. First, SWCNTs were placed in 2.6 M HNO_3 to reflux for 12 h. Then, they were sonicated in strong acid solution containing H_2SO_4 and HNO_3 (3:1 V/V) for 4 h at 0 °C after being washed to neutral with ice water and dried. Last, the filtered residue was washed with water to neutral and dried at 90 °C. After these treatments, the SWCNTs were cut to be shorter and much carboxyl emerged on their ends.

DA (3-hydroxytyramine hydrochloride) was obtained from Fluka. AA (L-ascorbic acid) was purchased from Beijing Chemical Reagent Co. Ltd. (China). UA was purchased from Merck. All other chemicals were analytical grade and used without further purification. All aqueous solutions were prepared with triply distilled water. Highly pure nitrogen gas was used for deaeration before electrochemical measurement.

2.3. The preparation of EDA-GCE

The fabricating process is briefly illustrated in Fig. 1. First, prior to modification, the bare GCE needs to be polished to mirror smoothness with 0.3 and 0.05 μm alumina slurry and residual alumina powder was removed by sonicating the electrode in ethanol and triply distilled water for 2 min, respectively. Then the well-polished GCE was electrochemically activated in 0.5 M H_2SO_4 using CV with the potential scan ranging from −1.0 to +1.0 V at the scan rate of 100 mV s^{-1} until a stable cyclic voltammogram was obtained. Afterwards, the electrode was oxidized in the solution containing 2.5% $K_2Cr_2O_7$ and 10% HNO_3 (wt%) using potentiostatic method at +1.5 V for 15 s. Second, the carboxylated GCE was washed and immersed in 0.1 M KCl solution containing 5 mM EDA, and CV was implemented for 40 cycles in the range of 0 to +1.9 V at the desired scan rate.

2.4. Fabrication of ace-pretreated SWCNTs array-GCE

The EDA-GCE was washed ultrasonically in triply distilled water and ethanol to remove the free EDA moleculars adsorbed on the electrode surface. After that, the electrode was immersed in aqueous KCl solution containing 0.4 g L^{-1} carboxylated SWCNTs which had been previously sonicated for 1 min. Finally, CV was implemented for 40 cycles in the range of 0 to +1.9 V at the desired scan rate, thus a SWCNTs array-GCE was prepared, and it would become a so-called Ace-pretreated SWCNTs array-GCE if SWCNTs array-GCE being ultra-sonicated with acetone for a given time before electrochemical measurement.

3. Results and discussion

3.1. Mechanism of dopamine oxidations

Dopamine oxidations have been thoroughly researched [14,33–35]. Basically, dopamine undergoes a well-known series of reactions classified as an electron transfer - chemical reaction - electron transfer (ECE) mechanism, and its reaction pathway is summarized in Fig. 2. Briefly, there are two chemical reactions interposed among three electrochemical reactions. The overall reaction is dominated by ring closure and rearrangement. Electrochemical Reaction 1 is the two-electron oxidation of dopamine (DA) to dopaminequinone (DAQ), which can undergo follow-up ring closure reaction leading to leucodopaminechrome (LDAC). LDAC can be in turn oxidized to dopaminechrome (DAC) through Electrochemical Reaction 2. After that, DAC maybe rearrange to 5,6-dihydroxyindole (DHI), which is further oxidized to indole-5,6-quinone (IQ) through Electrochemical Reaction 3. Though the redox peaks due to Electrochemical Reaction 1 and 2 have been recognized at all kinds of electrode, most researchers prefer the first redox peak to the second one when detecting DA because the latter is smaller and broader than the former. As far as the redox peaks due to Electrochemical Reaction 3 is concerned, it is always very difficult to trace any steps after Electrochemical Reaction 1 and 2. However, Muguruma et al. observed a barely discernible peak at long-length CNTs modified electrode [33]. Yong et al. also detected such an oxidation peak only at pH 7.68 and a temperature of 35 °C [35].

3.2. Electrochemical characteristics of DA at various GCEs

The fabrication of Ace-pretreated SWCNTs array-GCE covers five kinds of electrodes altogether. To characterize the influence of the electrode on DA oxidations, we used CV to record electrochemical signals with a Bare GCE and compared them to signals recorded by other electrodes that were modified either with EDA, SWCNTs alone or with SWCNTs array. As shown in Fig. 3, only one pair of redox peaks due to DA⇌DAQ at about 0.15 V could be clearly observed for Bare GCE, Carboxylated GCE and EDA-GCE. For all SWCNTs-based electrodes, another pair of redox peaks due to LDAC⇌DAC at about −0.26 V appeared obviously, showing a worse Faraday response. Furthermore, the third oxidation peak due to DHI⇀IQ at about 0.07 V (*arrow*) could be observed only for Ace-pretreated SWCNTs array-GCE.

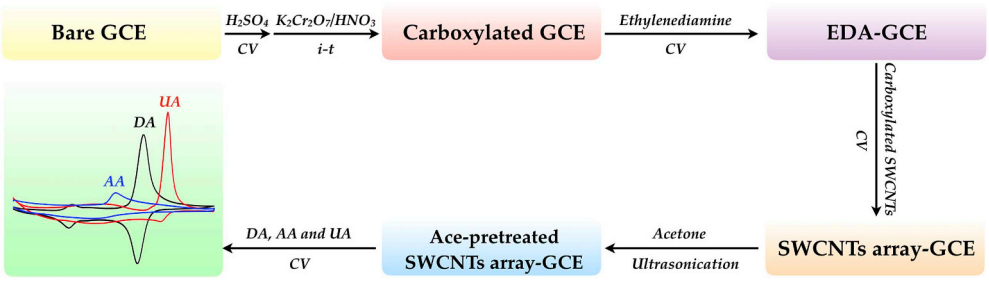

Fig. 1. Schematic representation of the fabrication of Ace-pretreated SWCNTs array-GCE.

Compared with Bare GCE, the first oxidation peak current of DA (at about 0.15 V) was around 1.5, 2.2, 5.0, 6.7 and 8.6 times higher at Carboxylated GCE, EDA-GCE, SWCNTs modified GCE, SWCNTs array-GCE and Ace-pretreated SWCNTs array-GCE, respectively. Excerpt 131 mV for Bare GCE, most of the peak potential separation were found to be in range of 60–70 mV, and which decreased to 44 mV particularly at Ace-pretreated SWCNTs array-GCE. The above results clearly indicated the catalytic DA oxidation at these modified electrodes.

The observations of peak current increasing in sequence and peak potential separation decreasing at Ace-pretreated SWCNTs array-GCE compared to that of the other modified electrodes may be attributed as follows. At pH 7.4, most DA molecules ($pK_b = 8.9$) exist as the cationic form. Meanwhile, there are negatively charged carboxyl groups on the Carboxylated GCE surface. As a consequence, the electrostatic attraction and hydrogen bonds exist between DA and carboxyl groups, which improve the response of DA. After the next step of EDA modification, phenolic hydroxyl groups of DA can form hydrogen bonds with amino groups of EDA, though they are positively charged leading to a little electrostatic repulsion. Considering the electrocatalytic ability to DA, SWCNTs modified GCE prepared with drop-casting pales in comparison to SWCNTs array-GCE. Actually, the SWCNTs loading at the former electrode surface is much more than the latter. That further confirms the superiority of the proposed modifying method that the utilization of SWCNTs is increased greatly. Especially, in the case of Ace-pretreated SWCNTs array-GCE, not only the electrochemical responses of DA is further improved, but also a rare third oxidation peak appears. We suppose a pretreatment with acetone can remove some impurities on the surface of SWCNTs array-GCE, which maybe include residual EDA or SWCNTs and so on.

3.3. Effect of Ace-pretreatment on SWCNTs array-GCE

We use CV, EIS and AFM to investigate the effect of Ace-pretreatment on SWCNTs array-GCE. There is only one pair of peaks due to the redox between DA and DAQ when the first CV scan is performed because only DA exists in the solution (not shown). Basically, in the following consecutive CV scans, DAQ still has two reaction pathway: one is reduced to DA, the other is cyclizing via deprotonation with its amine side chain to produce LDAC. So there are two pairs of peaks appearing (Fig. 4A). Interestingly, we can see trends for the produced DAC in similar situation: one is reduced to LDAC, the other is rearranging to form DHI which can be oxidized to IQ. Depending on various conditions such as electrode characteristic, potential scan rate, pH and temperature, it is very difficult to observe the redox peaks of DHI to IQ, even for SWCNTs

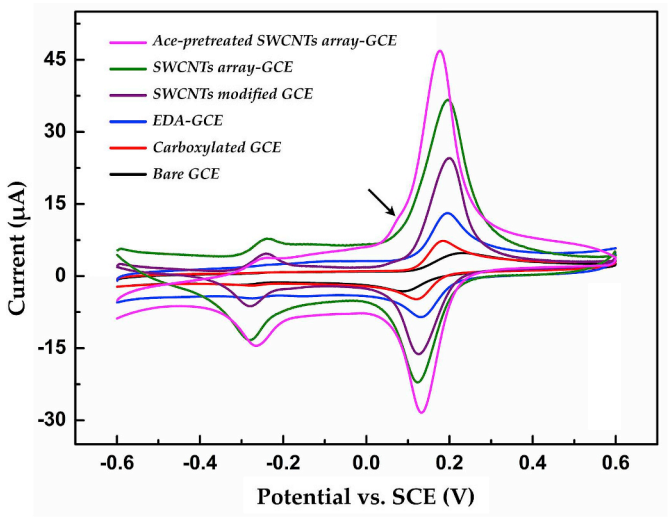

Fig. 3. Cyclic voltammograms of 0.2 mM DA in 0.1 M PBS (pH 7.4) at various GCEs. Scan rate: 100 mV s^{-1}.

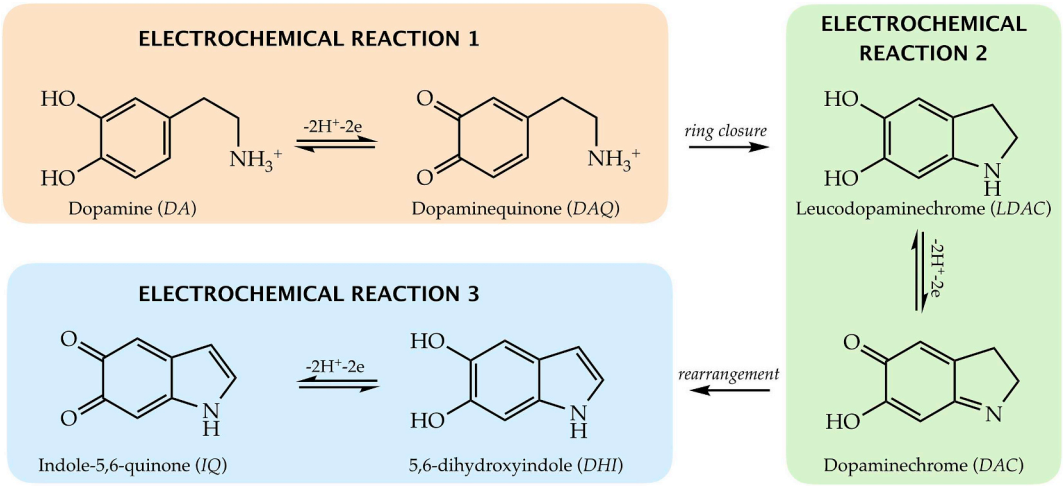

Fig. 2. Mechanism of dopamine oxidations.

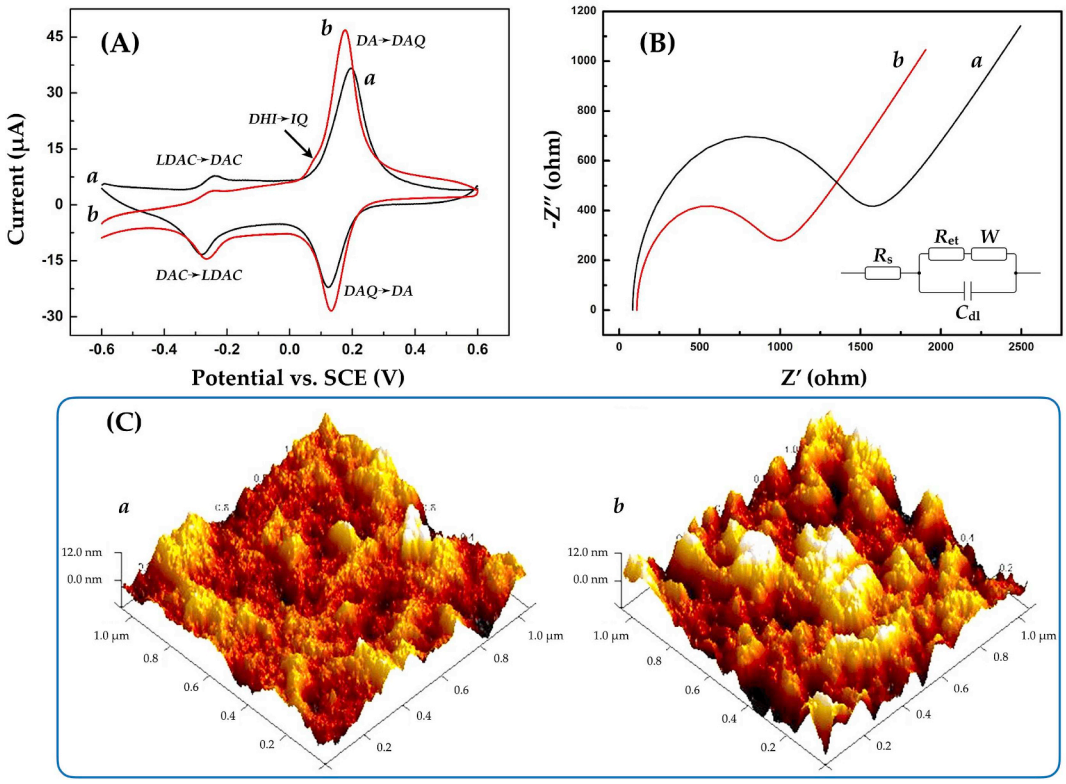

Fig. 4. Effect of Ace-pretreatment on SWCNTs array-GCE. "*a*" and "*b*" denote "*before*"and "*after*"Ace-pretreatment, respectively. (A) Cyclic voltammograms of 0.2 mM DA in 0.1 M PBS (pH 7.4). Scan rate: 100 mV s^{-1}. (B) Nyquist diagram of electrochemical impedance spectra in 5.0 mM $Fe(CN)_6^{3-/4-}$ solution. Initial potential: −0.001 V; frequency range: 0.1 Hz - 100 kHz; signal amplitude: 5 mV. Inset is the equivalent circuit of diffusion control type. (C) Atomic force microscopic tapping mode images.

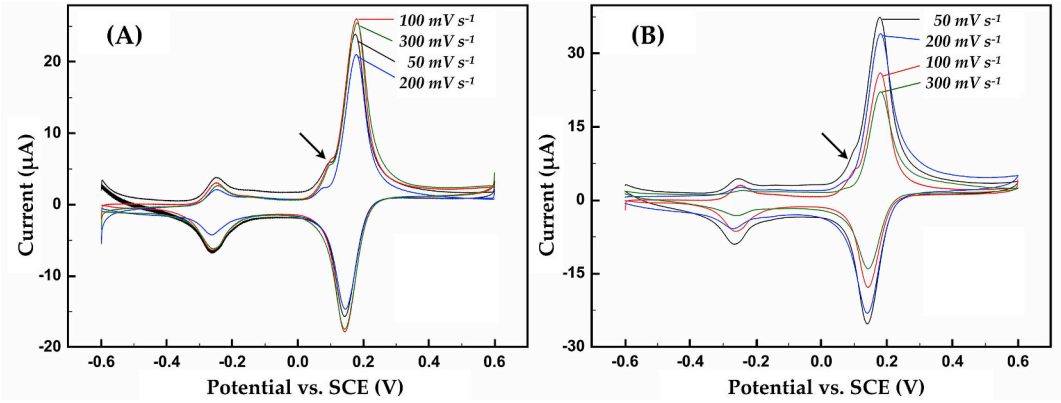

Fig. 5. Cyclic voltammograms of 0.2 mM DA in 0.1 M PBS (pH 7.4) at Ace-pretreated SWCNTs array-GCE fabricated by various modifying CV scan rates. (A) EDA modifying CV scan rate is varied while SWCNTs one is fixed at 100 mV s^{-1}. (B) SWCNTs modifying CV scan rate is varied while EDA one is fixed at 100 mV s^{-1}.

array-GCE. After Ace-pretreatment, the peak height of DA⇌DAQ increases while that of LDAC⇌DAC decreases slightly. As such, there are adequate amounts of DHI formed via rearrangement, thus leading to a clearly observable peak (arrow).

Fig. 4B shows typical impedance spectra in the form of Nyquist plots for SWCNTs array-GCE before and after Ace-pretreatment. The inset equivalent circuit is selected to fit the impedance data, where R_s, R_{et}, W and C_{dl} is the solution resistance, electron transfer resistance, Warburg impedance and double-layer capacitance, respectively. The R_{et} of SWCNTs array-GCE after Ace-pretreatment (770 Ω) is smaller than that before Ace-pretreatment (1300 Ω), suggesting a faster electron transfer kinetics of $[Fe(CN)_6]^{3-/4-}$ anions on the Ace-pretreated electrode.

Fig. 4C shows tapping mode AFM images of SWCNTs array-GCE before and after Ace-pretreatment. The observed morphology of electrode surface changed after Ace-pretreatment. The surface roughness increased resulting from more of the catalytic sites of CNTs exposed, and thus favoring the electrochemical reaction of DA. Like a surface detergent, acetone can clear all kinds of impurities on the electrode surface, most of which are adsorbed EDA and entangled CNTs.

3.4. Effect of modifying CV scan rate on SWCNTs array-GCE

We have developed an optimal method to prepare SWCNTs array-GCE in our previous paper [32]. This work aims to fabricate a sensitive sensor for DA, UA and AA detections. So it is necessary to adjust some modifying parameters in order to satisfy the new requirements. Since EDA and SWCNTs were successively connected to GCE by CV scan, CV

scan rate in modifying stage should have great effects on the performance of SWCNTs array-GCE. As shown in Fig. 5A, various EDA modifying CV scan rates (50–300 mV s^{-1}) have few effects on DA oxidation at SWCNTs array-GCE, indicating that EDA can be connected to carboxylated GCE easily and rapidly. In contrast, SWCNTs modifying CV scan rate has severely affected the performance of electrode. Theoretically, lower scan rate should be good for the forming of denser and more orderly SWCNTs. As to the peak currents due to DA⇌DAQ, they reached the maximum and the minimum when scan rate being 50 and 300 mV s^{-1}, respectively (Fig. 5B). But it is strange why the case of 200 mV s^{-1} excels that of 100 mV s^{-1}, and it needs further investigation. Based on our experimental results, 100 mV s^{-1} of EDA modifying CV scan rate and 50 mV s^{-1} of SWCNTs modifying CV scan rate are chosen.

3.5. DA, UA and AA oxidations at SWCNTs array-GCE

At Bare GCE, due to the sluggish oxidation of AA, its oxidation peak potential is more positive than that of DA (Fig. 6A). Between the two does the oxidation of UA occur. Because of their overlapping of the oxidation potentials and the catalytic oxidation of AA by DA, the electrochemical detection of DA in the presence of AA and UA is impossible by using Bare GCE. However, as shown in Fig. 6B, the sluggish oxidation of AA can be boosted by SWCNTs array, resulting in the eliminating of AA interference. Furthermore, the observation of peak currents increasing greatly imply that there should be a strong improvement in the electron transfer rate between SWCNTs array-GCE and DA. The same is true for AA or UA. Even their reversibility has also been improved in a way. We still choose the well-defined peak due to DA⇀DAQ as detection peak. The peak separation for AA-DA, DA-UA was about 170 mV and 144 mV, respectively, which should be large enough to selectively determine DA, UA or AA in the presence of the other two species, or simultaneously detect them in their mixture.

Further experiments were performed to study the electrochemical characteristics of DA, UA and AA at SWCNTs array-GCE under different scan rates. Both the DA and UA oxidation peak currents (i_{pa}, μA) were found to be directly proportional to the scan rates (υ, mV s^{-1}) ranging from 20 to 200 mV s^{-1}. The relations obey the following equations, i_{pa} (DA) = 0.289 υ – 2.97 (r = 0.9952) and i_{pa} (UA) = 0.393 υ – 11.2 (r = 0.9953), indicating a surface-controlled electrode process of DA or UA at SWCNTs array-GCE. DA can easily adsorb onto the electrode surface, and thus there was sufficient time for their oxidations. With regard to AA, the relationship between current and scan rate could be expressed as i_{pa} (AA) = 0.471 $\upsilon^{1/2}$–2.84 (r = 0.9920), suggesting that the oxidation of AA at SWCNTs array-GCE was diffusion-controlled mechanism.

3.6. Selective detection of DA or UA at ace-pretreated SWCNTs array-GCE

To explore the feasibility of the selective determination of DA, UA or AA at Ace-pretreated SWCNTs array-GCE, SWV was performed in their ternary mixture when the concentration of one species changed, whereas those of the other two species were kept constant. The optimal parameters for SWV was as follows: the increment of potential, frequency and amplitude are 4 mV, 10 Hz and 25 mV, respectively.

As shown in Fig. 7A, the calibration of DA was investigated in the presence of 0.2 mM AA and 0.16 mM UA. The peak current of DA increased with its concentration increasing. However, the effective level of the changes of DA concentration was different on the peak currents of AA and UA. The peak current of AA remained about the same even if DA concentration reached 100 μM, while that of UA decreased more than 5% if the coexisting DA concentration was larger than 2.0 μM. The calibration curve (inset of Fig. 7A) showed that the peak currents of DA increased linearly with concentrations in the range of 0.5–100 μM with a correlation coefficient of 0.9935 and a detection limit of 0.19 μM (S/N = 3).

Similarly, Fig. 7B showed the SWV responses of Ace-pretreated SWCNTs array-GCE toward the addition of UA with the different concentrations in the presence of 0.4 mM AA and 1.0 μM DA. As can be seen, the UA concentration can be effect on the peak currents of AA, but DA is not be affected. The oxidation peak currents of UA increased linearly with concentrations in the range of 0.01–0.2 mM with a correlation coefficient of 0.9930 and a detection limit of 0.82 μM (S/N = 3).

So far, the above experiments proved that the measuring scheme realize the selective detection for DA and UA, not being disturbed by each other and coexisting AA. But we could not get a satisfied linear relationship between AA peak current and its concentration because the presence of DA and UA both caused interference. The disturbance from UA can be predictable as AA peak current could be affected by UA (Fig. 7B). It is strange why DA has effect on the quantifying of AA but not the converse. We suppose that the third oxidation due to DHI→IQ maybe contribute to the apparent peak current of AA, and this effect is more serious especially in detecting low concentration of AA.

3.7. Analysis of DA and UA in real biological samples

In order to verify the reliability of the method for analysis of DA and UA in real samples, this Ace-pretreated SWCNTs array-GCE was applied to determine DA in human serum and UA in human urine samples by standard addition method. Both of the serum and urine samples were diluted with 0.1 M PBS (pH 7.4) before measurements, and then were directly determined using SWV technique. The analytical results are

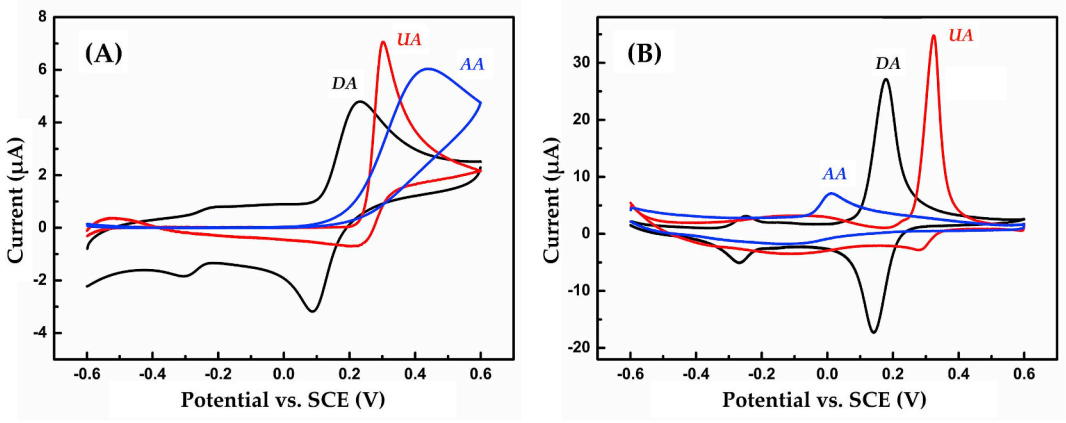

Fig. 6. Cyclic voltammograms of 0.2 mM DA or 0.4 mM AA or 0.2 mM UA in 0.1 M PBS (pH 7.4) at Bare GCE (A) and SWCNTs array-GCE (B). Scan rate: 100 mV s^{-1}.

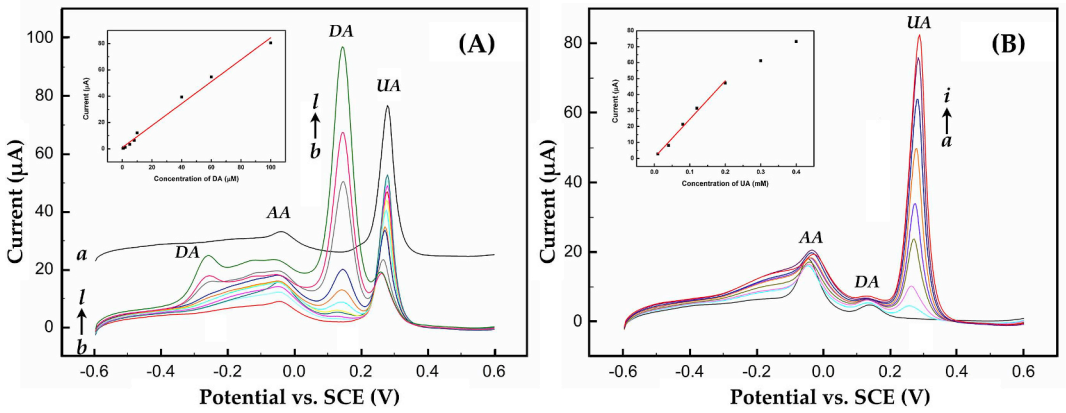

Fig. 7. (A) Square wave voltammograms of DA with 0.2 mM AA and 0.16 mM UA at Ace-pretreated SWCNTs array-GCE in 0.1 M PBS (pH 7.4). The concentration of DA (μM): (a) 0, (b) 0.2, (c) 0.5, (d) 0.8, (e) 1.0, (f) 2.0, (g) 5.0, (h) 8.0, (i) 10, (j) 40, (k) 60, (l) 100. (B) Square wave voltammograms of UA with 1.0 μM DA and 0.4 mM AA at Ace-pretreated SWCNTs array-GCE in 0.1 M PBS (pH 7.4). The concentration of UA (mM): (a) 0, (b) 0.01, (c) 0.04, (d) 0.08, (e) 0.12, (f) 0.20, (g) 0.30, (h) 0.40, (i) 0.50.

Table 1
Experimental results for the determination of DA in serum and UA in urine.

Sample	Target	Detected (μM)	Spiking (μM)	Found (μM)	RSD (%)	Recovery (%)
Serum	DA	–	70.8	71.8	1.5	101.4
		–	74.5	70.6	4.4	94.8
		–	78.0	76.7	1.8	98.3
Urine	UA	45	133	185	2.9	103.9
		80	135	210	1.6	97.7
		70	144	213	0.76	99.5

summarized in Table 1. The good recovery of DA and UA indicated that the proposed method could be effectively used for the determination of UA in real biological samples. Unfortunately, the concentration of DA in conventional biological samples like serum is too low to detect it directly, but it should be promising by using samples with higher concentration of DA like cerebrospinal fluid or by the means of enriching DA.

4. Conclusions

In conclusion, a novel SWCNTs array-GCE with EDA as a linker was fabricated successfully through a simple CV technique and was applied for sensitive and selective determination of DA and UA in their mixture. This modified electrode significantly improved the effective utilization of CNTs, and Ace-pretreatment could make a further improvement in the electrochemical response of DA, which was shown by the fact that a third two-electron oxidation of 5,6-dihydroxyindole to indole-5,6-quinone during DA oxidations can be clearly observed at the as-prepared modified electrode. This sensor was applied to the determination of UA and DA in real samples with satisfactory results. These characteristics including simple fabricating technique, inherent electrocatalytic activity and high availability of CNTs make SWCNTs array-GCE a useful analytical tool and could find broad potential applications in electrochemical sensors and biosensors.

Acknowledgements

This work was supported by the National Natural Science Foundation of China (Grant No. 21775007; 21475002 and 21335001) and the National Key Research and Development Program of China (Grant No. 2016YFA0201300).

References

[1] R.M. Wightman, L.J. May, A.C. Michael, Anal. Chem. 60 (1988) A769.
[2] S. Ramakrishnan, K.R. Pradeep, A. Raghul, R. Senthilkumar, M. Rangarajan, N.K. Kothurkar, Anal. Meth. UK 7 (2015) 779–786.
[3] J.W. Oh, Y.W. Yoon, J. Heo, J. Yu, H. Kim, T.H. Kim, Talanta 147 (2016) 453–459.
[4] J. Huang, Y. Liu, H. Hou, T. You, Biosens. Bioelectron. 24 (2008) 632–637.
[5] A.T. Lawal, Mater. Res. Bull. 73 (2016) 308–350.
[6] M. Stoytcheva, R. Zlatev, Z. Velkova, V. Gochev, G. Montero, L. Toscano, A. Olivas, Curr. Anal. Chem. 13 (2017) 89–103.
[7] R. Ramachandran, T. Chen, S. Chen, G.P.G. Kumar, M. Chinnasamy, N.B. Devi, T. Tseng, Int. J. Electrochem. Soc. 12 (2017) 1572–1588.
[8] S.M. Ghoreishi, M. Behpour, S. Mousavi, A. Khoobi, F.S. Ghoreishi, RSC Adv. 4 (2014) 37979–37984.
[9] S.R. Ali, Y.F. Ma, R.R. Parajuli, Y. Balogun, W.Y.C. Lai, H.X. He, Anal. Chem. 79 (2007) 2583–2587.
[10] S. Zhu, H. Li, W. Niu, G. Xu, Biosens. Bioelectron. 25 (2009) 940–943.
[11] Y.X. Li, X.Q. Lin, Sensor. Actuator. B Chem. 115 (2006) 134–139.
[12] J. Huang, D. Wang, H. Hou, T. You, Adv. Funct. Mater. 18 (2008) 441–448.
[13] A. Salimi, H. MamKhezri, R. Hallaj, Talanta 70 (2006) 823–832.
[14] Y.F. Zhao, Y.Q. Gao, D.P. Zhan, H. Liu, Q. Zhao, Y. Kou, Y.H. Shao, M.X. Li, Q.K. Zhuang, Z.W. Zhu, Talanta 66 (2005) 51–57.
[15] Y. Zhang, P. Xu, Q. Zeng, Y. Liu, X. Liao, M. Hou, Mater. Sci. Eng. C 74 (2017) 62–69.
[16] D.M. Fernandes, M. Costa, C. Pereira, B. Bachiller-Baeza, I. Rodriguez-Ramos, A. Guerrero-Ruiz, C. Freire, J. Colloid Interface Sci. 432 (2014) 207–213.
[17] H. Hu, Y. Song, M. Feng, H. Zhan, Electrochim. Acta 190 (2016) 40–48.
[18] M. Mazloum-Ardakani, H. Beitollahi, B. Ganjipour, H. Naeimi, M. Nejati, Bioelectrochemistry 75 (2009) 1–8.
[19] J. Li, W.Z. Wei, S.L. Luo, Microchim. Acta 171 (2010) 109–116.
[20] M. Noroozifar, M. Khorasani-Motlagh, M.B. Parizi, R. Akbari, Ionics 19 (2013) 1317–1327.
[21] A. Gutierrez, A. Gasnier, M.L. Pedano, J.M. Gonzalez-Dominguez, A. Anson-Casaos, J. Hernandez-Ferrer, L. Galicia, M.D. Rubianes, M.T. Martinez, G.A. Rivas, Electroanalysis 27 (2015) 1565–1571.
[22] G.B. Li, J.C. Hao, J. Electrochem. Soc. 156 (2009) K134–K138.
[23] L. Chen, F. Chang, L. Meng, M. Li, Z. Zhu, Analyst 139 (2014) 2243–2248.
[24] Z. Lu, W. Xu, J. Ma, Y. Li, X. Sun, L. Jiang, Adv. Mater. 28 (2016) 7155–7161.
[25] E. Penzo, M. Palma, D.A. Chenet, G. Ao, M. Zheng, J.C. Hone, S.J. Wind, ACS Nano 10 (2016) 2975–2981.
[26] B. Endrodi, G.F. Samu, D. Fejes, Z. Nemeth, E. Horvath, A. Pisoni, P.K. Matus, K. Hernadi, C. Visy, L. Forro, C. Janaky, J. Polym. Sci., Polym. Phys. Ed. 53 (2015) 1507–1518.
[27] E. Penzo, M. Pama, R. Wang, H. Cai, M. Zheng, S.J. Wind, Nano Lett. 15 (2015) 6547–6552.
[28] C. Yang, C.B. Jacobs, M.D. Nguyen, M. Ganesana, A.G. Zestos, I.N. Ivanov, A.A. Puretzky, C.M. Rouleau, D.B. Geohegan, B.J. Venton, Anal. Chem. 88 (2016) 645–652.
[29] D. Mandler, S. Kraus-Ophir, J. Solid State Electrochem. 15 (2011) 1535–1558.
[30] M. Engel, J.P. Small, M. Steiner, M. Freitag, A.A. Green, M.C. Hersam, P. Avouris, ACS Nano 2 (2008) 2445–2452.
[31] C.M. Crudden, J.H. Horton, I.I. Ebralidze, O.V. Zenkina, A.B. McLean, B. Drevniok, Z. She, H. Kraatz, N.J. Mosey, T. Seki, E.C. Keske, J.D. Leake, A. Rousina-Webb, G. Wu, Nat. Chem. 6 (2014) 650-650.
[32] H. Zhu, F.X. Chang, Z.W. Zhu, Talanta 166 (2017) 70–74.
[33] H. Muguruma, Y. Inoue, H. Inoue, T. Ohsawa, J. Phys. Chem. C 120 (2016) 12284–12292.
[34] M.D. Hawley, S.V. Tatawawadi, S. Piekarski, R.N. Adams, J. Am. Chem. Soc. 89 (1967) 447–450.
[35] T.E. Young, B.W. Babbitt, J. Org. Chem. 48 (1983) 562–566.